Paper No.
PPU25

CORCON
17-20 September
Mumbai, India
2017

Corrosion of Nickel alloys in molten LiCl-KCl medium under Cl_2 environment

A. Ravi Shankar
Corrosion Science and Technology Division,
Indira Gandhi Centre for Atomic Research, Kalpakkam – 603102, India
rshankar@igcar.gov.in

U. Kamachi Mudali
Materials Chemistry & Metal Fuel Cycle Group,
Indira Gandhi Centre for Atomic Research, Kalpakkam – 603102, India

ABSTRACT

Pyrochemical reprocessing utilising molten chloride salt medium has been considered as one of the best options for the reprocessing of spent metallic fuels of future fast breeder reactors. Purification of molten salt is an important step, where chlorine gas is purged in molten LiCl–KCl eutectic salt at 873 K which is a highly corrosive environment. The materials used for fabrication of vessels and components of salt purification system should therefore possess adequate corrosion resistance. Corrosion studies on Ni-based alloys 600 (UNS N06600), 625 (UNS N06625), and 690 (UNS N06690) and their welds in molten LiCl–KCl eutectic salt at 873 K under Cl_2 bubbling was carried out. The exposed surfaces were characterised using SEM, EDX and GIXRD. The results of the present study indicated that Ni-based alloy 600 and 690 offered better corrosion resistance compared to alloy 625. Localised corrosion and selective attack such as intergranular corrosion and preferential dissolution of precipitates within the grain were observed on the alloy 600 and alloy 625. However, weldments exhibited marginally higher corrosion rate compared to wrought alloy. Surface morphology of the tested weld metal surfaces revealed interdendritic corrosion on alloy 600 and alloy 625. The mechanism of degradation of Ni base alloys in molten LiCl-KCl salt under chlorine gas was found to be different from that observed in air and argon environment. It involved active oxidation process, resulting in accelerated corrosion under chlorine gas.

Keywords: Molten Salt Corrosion, Ni base alloys, Chlorine, SEM

INTRODUCTION

Pyrochemical reprocessing involves the use of molten salt and molten cadmium for the recovery of uranium, plutonium from spent metallic fuel (U-Pu-Zr) of future fast breeder reactors.[1] Salt purification is the first and foremost important step in pyrochemical reprocessing. In this process the impure molten salt containing oxygen and moisture is purified by bubbling chlorine gas into molten salt at 773 to 873 K. Corrosion is an important issue during salt purification as the high temperature molten salt containing oxygen, moisture and chlorine gas is highly corrosive. Material selection is therefore vital for successful operation of the salt purification system and the material selected should have reasonably good corrosion resistance, to avoid contamination of the salt. Therefore materials testing and selection for manufacturing of vessels and components for salt purification system are of paramount importance. There is limited literature available on corrosion of structural materials in molten salt under chlorine bubbling. It is reported that Ni-rich alloys experience less attack in chlorine-containing environments than carbon steels and stainless steel.[2] It is postulated that nickel base alloys are more resistant than steels because the Gibbs free energy change of $FeCl_2$ formation is less negative than that of $NiCl_2$ formation and the partial pressure of nickel chloride is significantly lower than partial pressure of iron chlorides.[3] Corrosion studies carried out on various materials in molten $NaCl-KCl-CsCl-UO_2Cl_2$ salt for 6 h at 873 and 923 K under O_2 and Cl_2 gases showed that the corrosion rate of ZrO_2-SiO_2 is less than that of pyrolytic graphite.[4] Takeuchi et al.[5] showed that Si_3N_4, $Al_6Si_2O_{13}$ and $Mg_2A_{l3}(AlSi_5O_{18})$ exhibit better corrosion resistance than pyrolytic graphite in molten NaCl-KCl salt under Cl_2 bubbling at 1023 K for 24 h. For the engineering scale salt purification system at Indira Gandhi Centre for Atomic Research (IGCAR), INCONEL† 600 was used for the fabrication of outer vessel with high density (HD) graphite as an inner liner. Limited literature exists on corrosion of alloys, ceramics and graphite in molten chloride salt under Cl_2 bubbling. Therefore candidate materials like INCONEL† 600 (UNS N06600), INCONEL† 625 (UNS N06625) and INCONEL† 690 (UNS N06690) and their welds were evaluated in molten LiCl–KCl eutectic salt at 873 K under chlorine bubbling.

EXPERIMENTAL PROCEDURE

SAMPLE PREPARATION

The chemical composition of the alloys tested in the present study is shown in Table 1. Samples of size 50 x 12 x 5 mm were cut from the plate stock and polished upto 1200 grit emery paper for corrosion testing. Autogenous weld samples of INCONEL† 600, 625 and 690 samples were prepared and subjected to radiographic examination (BALTOGRAPH) as per ASME SEC III DIV I. Weld samples for corrosion testing were prepared from defect free regions of autogenous weld pads. Defect free samples from the weldment of size 50 x 12 x 5 mm similar to the base metal were cut from the welded plate and polished for corrosion studies. The samples were cleaned with distilled water and then with acetone and dried before corrosion test.

Table 1: Chemical composition of as-received alloys in wt%.

Material	Ni	Cr	Fe	Mn	Si	Mo	Ti	Ta+Nb
INCONEL† 600	72	17	10	1	-	-	-	-
INCONEL† 625	64	21.5	4.25	-	-	9	-	3.15
INCONEL† 690	60	29.58	9.05	0.21	0.25	-	0.2	0.02

MOLTEN SALT CORROSION EXPERIMENT

The schematic diagram of quartz chlorination cell used for corrosion testing in molten LiCl-KCl salt under Cl_2 bubbling is shown in Figure 1. Experiments were carried out by immersing the samples inside the alumina crucible containing salt and chlorine bubbling. In order to study the combined effect of Cl_2 bubbling and molten salt (aggressive conditions), samples were suspended in the molten salt as shown in Figure 1. An INCONEL† 600 plate sample (base metal) and INCONEL† 600 weldment sample was fixed to the alumina sleeve sample holder. Samples were fixed to the sample holder using threaded joint by providing internal thread to the sample and external thread to the sample holder. The samples were immersed into the molten salt by lowering the sample holder. As-received LiCl-KCl salts contain moisture and oxygen as they are hygroscopic in nature. In order to eliminate these impurities and purify the salt, vacuum drying and subsequent chlorination of the salt is being carried out by Cl_2 bubbling. Vacuum dried LiCl-KCl (44.48 wt% LiCl – 55.52 wt% KCl) eutectic salt transferred to an alumina crucible was placed inside the chlorination cell as shown in Figure 1.

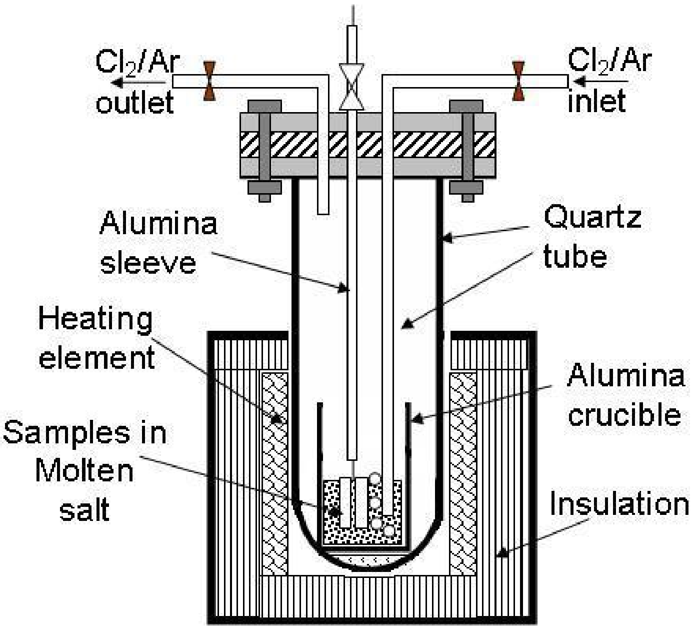

Figure 1: Schematic diagram of chlorination cell and furnace used for corrosion testing, depicting samples immersed in molten LiCl-KCl salt under Cl_2 bubbling

Around 100 g of salt was loaded for each experiment into the cell along with samples. After loading salt in to the cell, sealing of the cell was done to avoid pickup of oxygen and moisture in to the salt. The sealed cell containing samples and salt was then placed in the furnace and heated under argon atmosphere upto 873 K. After reaching the desired temperature, the samples were lowered in the molten salt. The samples were lifted/withdrawn from the molten salt after 30 minutes of Cl_2 bubbling. Salt purification in pyrochemical reprocessing is usually carried out by Cl_2 bubbling for 30 minutes in the molten salt. Therefore in order to simulate plant conditions samples were immersed in molten salt under Cl_2 bubbling for 30 minutes. Similarly, corrosion experiments were carried out on INCONEL† 625 and its weld, INCONEL† 690 and its weld, in molten LiCl-KCl salt under Cl_2 bubbling for 30 minutes. After the corrosion test, samples were removed and cleaned with distilled water and then ultrasonically cleaned with acetone and dried. The weights of the samples were noted before and after the corrosion test and weight losses were determined. The corrosion rates of the samples exposed to molten LiCl-KCl salt under Cl_2 bubbling were calculated as shown in Equation (1)[6]

Corrosion rate (mm/year) = $(8.76 \times 10^4 \times W) / (A \times D \times T)$ -------- (1)

Where: T = time of exposure in h, A = total surface area in cm^2, W = weight loss in g, and D = density of the sample, g/cm^3.

These experiments under highly toxic and corrosive Cl_2 environment simulate the salt purification process and provide valuable information for material selection and associated corrosion mechanisms involved.

CHARACTERISATION OF SAMPLES

The surface morphology and compositional analysis of corroded surfaces were carried out using ESEM Philips XL-30 scanning electron microscopy (SEM) attached with EDX (Energy Dispersive analysis of X-rays). Glancing Incidence X-ray Diffraction (GIXRD) was carried out with 2 step size of 0.1 degree and with time per step as 7 sec, using STOE diffractometer on the corroded surfaces. The incidence angle used for GIXRD measurements was 0.5 degree. Powder Diffraction File-2 was used for the phase analysis of the XRD patterns and PDF-2 codes[7] of the phases observed were provided in square brackets.

RESULTS AND DISCUSSION

Initial experiments carried out by immersing the samples in alumina crucible showed that the surface of the sample in contact with crucible experienced less corrosion attack than other surfaces. Moreover, the effect of Cl_2 bubbling on the corrosion behaviour was observed to be significantly less when the samples were immersed in the crucible. Therefore experiments were conducted by fixing samples to an alumina sleeve sample holder and immersing the samples into molten salt without contacting with alumina crucible by lowering the sample holder as shown in Figure 1. Corrosion rate of INCONEL† 600, 625 and 690 samples were found to be 1.32, 2.54, 0.99 mm yr^{-1} respectively while INCONEL† 600, 625 and 690 welds exhibited corrosion rates of 1.36, 2.90, 0.90 mm yr^{-1} respectively. The corrosion rate results indicated that INCONEL† 690 is better than INCONEL† 600 and INCONEL† 625. INCONEL† 625 showed the highest corrosion rate compared to INCONEL† 600 and INCONEL† 690. INCONEL† 625 weldment also exhibited marginally higher corrosion rate than the base metal. Indacochea et al.[8] reported that INCONEL† 625 performed poorly and had a serious

† Trade Name

reduction in mass, one-half of its original weight, and a significant decrease in thickness when tested in LiCl-3.5 wt% Li_2O at 923 K in argon + 10% oxygen atmosphere. In their study INCONEL† 600 showed better performance compared to INCONEL† 625 and the poor performance of INCONEL† 625 was attributed by Indacochea et al.[8] as a consequence of molybdenum and chromium present. The catastrophic attack induced by molybdenum in Fe and Ni base alloys during hot corrosion has been reported.[9] Catastrophic oxidation has been referred to a situation in which liquid phase is formed in the oxidation process.[10] It is reported that the melting point of $MoCl_5$ is 467 K[10] and that of mixed oxides of MoO_2-MoO_3, MoO_2-MoO_3-Cr_2O_3 and MoO_2-MoO_3-NiO were 1051, 1045 and 1037 K respectively.[11] The formation of these oxides results in enrichment of Mo, and subsequent formation of low melting phases results in breakaway of film, resulting in accelerated corrosion. In another study nickel molybdate (or tungstate) was identified in the scale and this induced formation of a highly friable and porous scale which was held to be largely responsible for the accelerated attack.[12] The accelerated attack of INCONEL† 625 in molten LiCl-KCl salt in the presence of Cl_2 observed in the present study could also be attributed to the presence of Mo, however, the lower oxygen contents (present in the salt) prevailing in the present experimental condition could indicate formation of majority of low melting Mo rich chlorides. Kim et al.[13] developed new alloy with composition similar to that of Inconel 713LC and reduced Si and Mo contents which exhibited better corrosion resistance in molten salt.

The surface morphology of INCONEL† 600, INCONEL† 625 and INCONEL† 690 samples exposed to molten LiCl-KCl salt in the presence of Cl_2 are shown in Figures 2a-c respectively. The surface morphology of INCONEL† 600 exhibited intergranular type of attack, while on INCONEL† 625 dense and porous regions were evident. The surface morphology of INCONEL† 690 exhibited more or less uniform attack. EDX measurements were made from the regions indicated in the micrographs and the results were tabulated in Table 2. From these results, it was evident that there was no marked difference in the chemical composition of various regions. This indicates that there is no thick scale formation and preferential enrichment or depletion of elements on the surface as could be resolved by EDX. This is contrary to the corrosion of 316L stainless steel and Ni base alloys tested in molten LiCl-KCl salt in air environment which exhibited distinct scales on the surface with enrichment of Cr on the surface and formation of Cr rich and Ni rich layers.[14.15] Earlier studies on 316L SS and Ni base alloys exposed to molten LiCl-KCl salt in air revealed selective outward diffusion of Cr and formation of chromium rich oxides at the surface and subsequent spallation of the scales formed.[14.15] Corrosion studies on Cr-Mo steels, stainless steels and Ni base alloys exposed to molten LiCl-KCl salt under ultra high purity (UHP) Ar atmosphere also indicated a similar type of attack[16.17], though the rate of attack is lower than in air environment. The present results suggest that the mechanism of degradation of Ni base alloys in molten LiCl-KCl salt under chlorine gas is different from that in air and argon environment. The nature of films formed on the surface of Ni base alloys might be low melting and soluble in molten salt under Cl_2 bubbling which resulted in much accelerated corrosion.

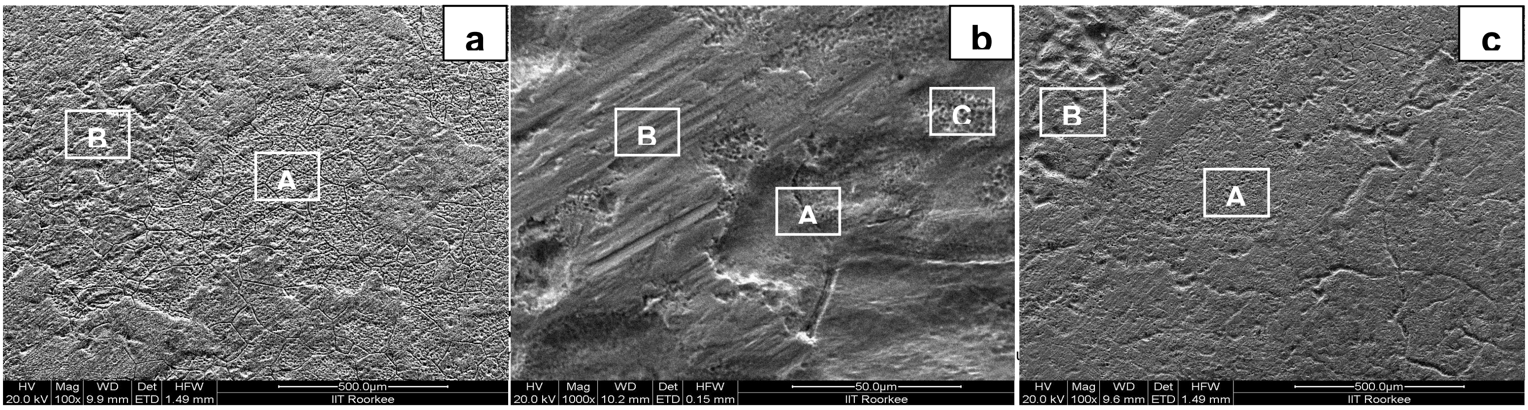

Figure 2: Surface morphology of samples exposed to molten LiCl-KCl salt in the presence of Cl_2 (a) INCONEL† 600 (b) INCONEL† 625 and (c) INCONEL† 690.

High temperature corrosion in molten salts often exhibits selective attack and internal oxidation. Selective attack of INCONEL† 600 was observed in molten chloride melts and the resulting attacked region consisted of layers of porous, sponge like morphology with pores generally not interconnected and typically located at the grain boundaries.[10] INCONEL† 713LC showed local corrosion behaviour and NIMONIC† 80A, NIMONIC† 90 showed uniform corrosion behaviour in molten LiCl-Li_2O salt.[18] The surface morphology of INCONEL† 600, INCONEL† 625 and INCONEL† 690 exposed to molten LiCl-KCl salt in the presence of Cl_2 are shown in Figures 3a-c respectively. The surface morphology of corroded INCONEL† 600 surface (Figure 3a) clearly revealed intergranular corrosion and preferential dissolution of precipitates within the grain.

Table 2: Chemical composition (in wt% by EDX) from regions shown in Figure 2 of various Ni based alloys after corrosion test.

Material	Region	Ni	Cr	Fe	Mn	Si	Al	Mo	Ta	O	Cl
INCONEL† 600	A	70.97	15.43	8.77	0.25	1.35	-	-	-	3.22	-
	B	70.22	15.98	8.37	0.53	1.03	-	-	-	3.87	-
INCONEL† 625	A	52.98	18.49	4.16	0.79	0.88	0.71	12.59	4.81	4.01	0.59
	B	51.33	18.41	3.68	0.52	1.17	0.78	14.22	3.72	4.42	1.76
	C	55.98	19.56	4.29	1.07	-	-	9.82	5.69	3.31	0.29
INCONEL† 690	A	61.24	28.34	2.67	-	0.14	3.53	-	-	4.07	-
	B	58.55	26.43	4.87	0.98	0.65	3.98	-	-	4.29	-

Similarly, the surface morphology of corroded INCONEL† 625 surface also exhibited intergranular corrosion (Figure 3b). The surface morphology of INCONEL† 690 (Figure 3c) on the other hand did not show any such localized attack. The surface morphology of INCONEL† 600 revealed selective dissolution of twin boundaries and predominant attack on twin boundaries was observed on INCONEL 625 apart from intergranular corrosion. INCONEL† 690 exhibited a porous morphology in contrast to other Ni base alloys. The localized intergranular attack and attack along twin boundaries could be attributed to the presence of Cr depleted regions around the carbide precipitates formed along these boundaries which make these regions more prone to corrosion than matrix. The preferential dissolution of precipitates observed could also be due to preferential attack of carbides leading to the formation of volatile species according to the Equation (2)[19] as explained below.

$M_7C_3 + 7\ Cl_2\ (g) + 3\ O_2\ (g) \quad 7\ MCl_2\ (g) + 3\ CO_2\ (g)$ -------- (2)

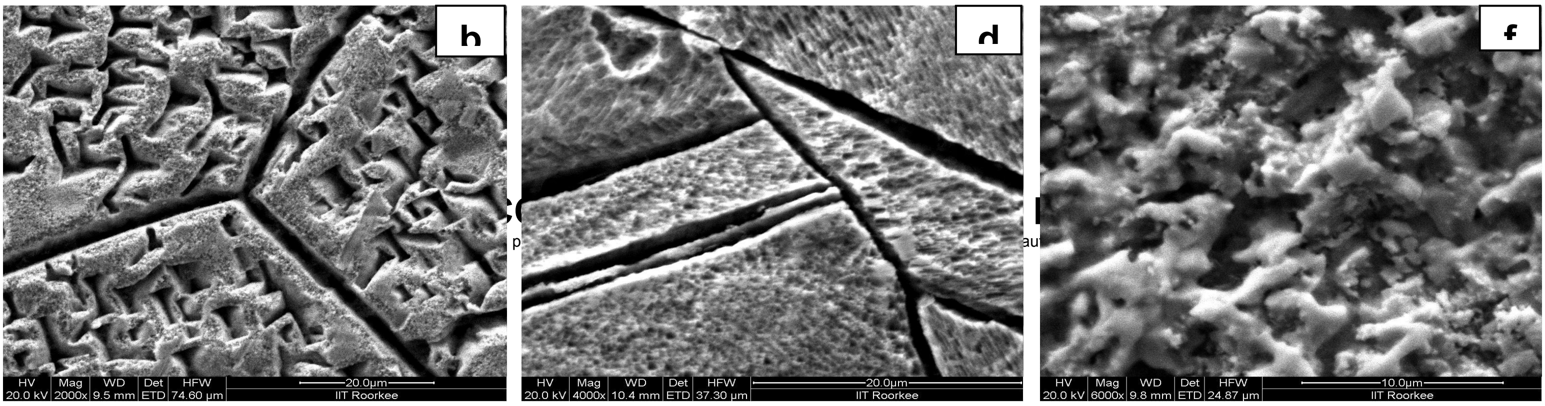

Figure 3: Surface morphology of samples exposed to molten LiCl-KCl salt in the presence of Cl_2 (a) INCONEL[†] 600 (b) INCONEL[†] 625 and (c) INCONEL[†] 690.

The surface morphology of weldments of INCONEL[†] 600, INCONEL[†] 625 and INCONEL[†] 690 exposed to molten LiCl-KCl salt in the presence of Cl_2 are shown in Figures 4a-c respectively. The surface morphology of INCONEL[†] 600 (Figure 4a) and INCONEL[†] 625 (Figure 4b) samples in the weld region revealed the dendritic structure present in the weld region. This indicates that cell boundaries and interdendritic boundaries undergone selective dissolution in the weld region for INCONEL[†] 600 and 625 respectively. The cell boundaries in INCONEL[†] 600 sample also undergone selective attack compared to the dendritic structure present within the cell (Figure 4a). These results clearly indicate that INCONEL[†] 600 and 625 exhibited localized attack while INCONEL[†] 690 (Figure 4c) exhibited uniform dissolution. It is reported that the welded portion of 316L SS coupon was also found to have corroded extensively in addition to significant intergranular corrosion attack observed in the heat affected zone and the base metal, when tested in LiCl with 3.5 wt% Li_2O for 6 days at 923 K in argon with 10% oxygen atmosphere.[8] These results suggest that weldments are prone to uniform as well as localised corrosion and fabrication techniques without welding or with optimized welding procedures are preferable for manufacturing of crucibles exposed to molten salt in the presence of chlorine gas.

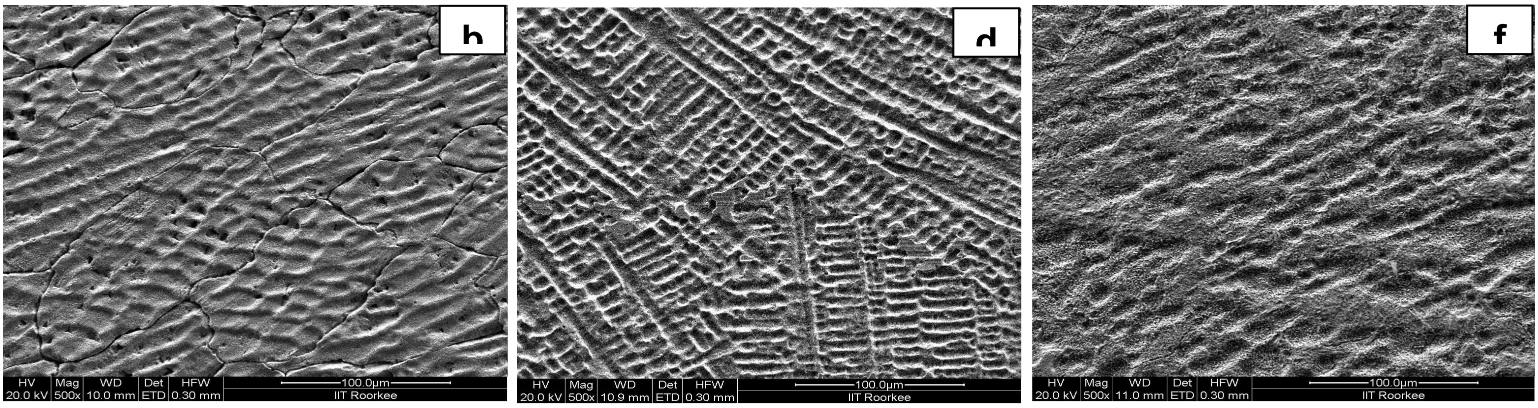

Figure 4: Surface morphology of welds of samples exposed to molten LiCl-KCl salt in the presence of Cl_2 (a) INCONEL[†] 600 (b) INCONEL[†] 625 and (c) INCONEL[†] 690.

A schematic illustration of active oxidation process at high temperatures in oxidizing/chloridizing environments as reported resulting in circulation of chlorine[19] with a simplified sketch is shown in Figure 5. Corrosion initially starts with dissolution of metal and formation of metal chloride as the Gibbs free energy of formation of metal chloride is negative. Due to low oxygen partial pressure at the metal/oxide interface, metal chlorides can form at the interface.[3] In oxidising atmosphere metal oxides are stable, therefore, metal chlorides oxidise to form metal oxides wherever oxygen is available. The scales/film become porous due to the precipitation of metal oxide in the existing oxide scale leading to massive growth stresses in the scale/film.[20] Thus the porous, brittle oxide scale spalls or cracks which allow easy transport of chlorides/chlorine/oxygen. The melting point of most of the chlorides are low compared to that of oxides, and if partial pressure of metal chlorides are significant, the metal chloride can diffuse outward[20] through pores and cracks present in the scale[3] and oxidise to form metal oxides. The chlorine thus released diffuses back to the substrate and

† Trade Name

results in fresh metal chloride formation.[3,20] Thus the process is catalysed by chlorine[20] and the active oxidation process continues as shown in the figure. Also, as shown in the figure the carbides get preferentially attacked leading to the formation of volatile metal chlorides and gaseous CO_2.[19] The volatile and gaseous products would further disrupt the scale/film exposing the fresh surface to corrode. The metal chlorides formed from carbide could also oxidise to form metal oxides depending on the oxygen availability and the released chlorine further catalyses the corrosion process. It is reported that intergranular attack of alloys in molten salt occurred along grain boundaries and lowering carbon content and decreasing grain size resulted in improvement.[21] INCONEL† 690 with lower carbon content has lower carbide precipitation compared to INCONEL† 600 and INCONEL† 625 and thus lesser localized attack along grain boundaries and twin boundaries in INCONEL† 690. From the carbides (Cr_xC_y) at grain boundaries, $CrCl_2$ could be formed and volatile $CrCl_2$ would be oxidized and results in the precipitation of Cr_2O_3 under Cl_2 and O_2 atmosphere.[19] In case of high Mo containing alloys, the formation of oxychlorides is reported to be particularly detrimental in oxidizing-chloridizing atmospheres.[22] Bender and Schutze[19] suggested that in order to keep corrosion rates low where formation of volatile metal chlorides takes place, the vapor pressure of the chlorides in the environments should not exceed a critical value of 10^{-4} bar. Therefore Ni base alloy with lower carbon content (to minimise carbide precipitation) and lower molybdenum content are preferable for molten LiCl–KCl salt medium in the presence of Cl_2.

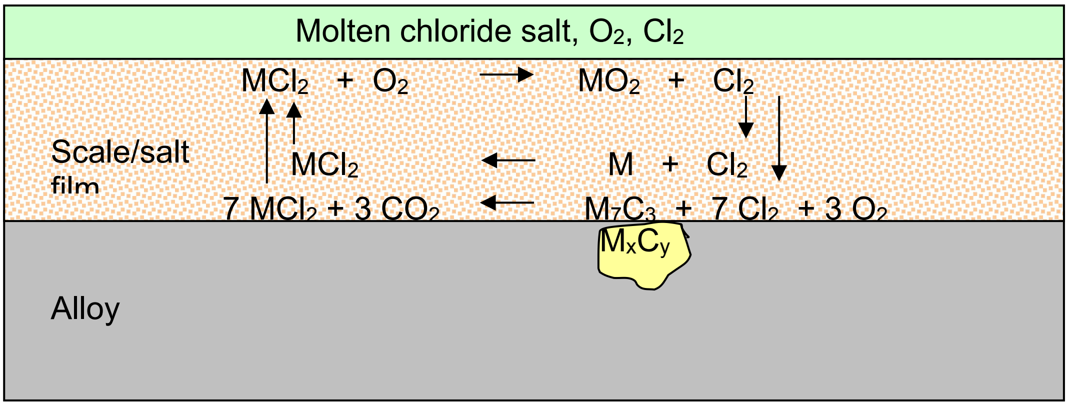

Figure 5: Schematic illustration of the mechanism of attack in oxidizing/chloridizing environments depicting substrate, salt and circulation of chlorine during active oxidation process.[19]

The cross section micrographs of corroded samples did not exhibit corrosion products, enriched and/or porous layers. These results also indicate that the corrosion products formed could be either volatile or soluble and therefore dissolved into the molten salt. The GIXRD pattern of corroded surface of INCONEL† alloys after corrosion test exhibited major reflections corresponding to austenite ($Fe_{0.7}Cr_{0.19}Ni_{0.11}$) [33-0397] phase on INCONEL† 690 and 625. The major Ni [04-0850] phase observed on INCONEL† 600 indicates that selective leaching/dealloying might have occurred on the surface leaving a Ni rich layer. However, EDX elemental composition did not reveal Ni enriched region on INCONEL† 600 surface. This indicates that a thin Ni enriched layer might have formed on INCONEL† 600 surface. During molten LiCl-KCl salt corrosion in air environment, scales formed got easily detached, and the XRD pattern of scales formed showed that Cr_2O_3 and NiO are the phases present in various proportions in all the scales and in addition spinel oxide $NiCr_2O_4$ was observed in the scale of INCONEL† 600 and alloy 800H.[14.15] Molten salt corrosion in chlorine environment did not result in the formation of such loosely adherent thick scales. Thus from the results of SEM-EDX, cross section SEM and GIXRD, it is clear that corrosion products formed are either volatile or soluble in molten LiCl-KCl under Cl_2 bubbling and resulted in severe uniform and localised corrosion. The lack of protective film formation and accelerated corrosion in this kind of aggressive environment necessitates the use of graphite liner or ceramic coatings for corrosion protection.

Compared to these Ni base alloys, high density graphite and Partially Stabilized Zirconia (PSZ) coating could exhibit better performance in molten LiCl-KCl salt under Cl_2 bubbling. Our earlier studies on PSZ coatings on candidate materials tested in molten LiCl-KCl salt under argon atmosphere exhibited excellent corrosion resistance.[16.23.24] These studies shows that pyrolytic graphite, high density graphite and ceramic coatings like alumina and PSZ on Ni base alloys could improve the performance of the components/vessels in molten LiCl-KCl salt under Cl_2 bubbling compared to bare alloys exhibiting undesirable corrosion rates. Takeuchi et al.[5] carried out weight loss studies on candidate ceramic materials in molten NaCl–KCl salt under Cl_2 bubbling at 750°C for 24 h. Their study revealed that alumina, beryllia, silicon nitride (Si_3N_4), mullite ($Al_6Si_2O_{13}$) and cordierite ($Mg_2Al_3(AlSi_5O_{18}$) showed good corrosion resistance than pyrolytic graphite. Similar corrosion studies in molten salt in the presence of fission product chlorides under Cl_2 and O_2 gas also revealed that silicon nitride, mullite and cordierite showed good corrosion resistance than pyrolytic graphite.[5] It is also essential to carry out corrosion studies on such ceramic materials in molten LiCl–KCl salt under Cl_2 bubbling for selection of corrosion resistant materials or coatings. Apart from this corrosion studies in molten salt in the presence of fission product chlorides need to be undertaken to study their effect on dissolution of structural materials.

The short time test carried out in the present study simulates the aggressive attack due to the presence of moisture and oxygen present in salt and chlorine bubbling during lab scale salt purification process. However, considering the practical difficulties in handling high temperature molten salt under highly toxic and lethal chlorine gas, long term corrosion studies are required to simulate engineering scale salt purification conditions to make concrete conclusions and understand the nature of attack and reactions taking place.

CONCLUSIONS

The following are the salient conclusions drawn from this study:

1. Corrosion tests performed on INCONEL† 600, INCONEL† 625, and INCONEL† 690 in molten LiCl–KCl salt under Cl_2 bubbling indicated that INCONEL† 690 showed better corrosion resistance compared to INCONEL† 600 and INCONEL† 625. The higher corrosion rate of INCONEL† 625 could be attributed to the development of Mo rich layers, catastrophic oxidation and breakaway.

2. The surface morphology of corroded INCONEL† 600 and INCONEL† 625 surface clearly revealed intergranular corrosion, corrosion along twin boundaries and preferential dissolution of precipitates within the grain. The surface morphology of INCONEL† 690 on the other hand did not show any such localized attack.

3. The surface morphology of weldments of INCONEL† 600 and 625 revealed cell boundary dissolution and interdendritic dissolution in the weld region respectively while uniform corrosion was observed on INCONEL† 690 weldment. The intergranular and interdendritic dissolution was

attributed due to Cr depleted regions around carbide precipitates or due to attack of carbide precipitates which led to preferential dissolution along these boundaries.

4. GIXRD analysis indicated no oxide scales/corrosion products on INCONEL† 600, INCONEL† 625 and INCONEL† 690 exposed to molten LiCl–KCl salt under Cl_2 bubbling unlike those formed in molten LiCl-KCl salt under air and UHP argon environment.

5. Protective ceramic coatings could provide better corrosion resistance in molten LiCl–KCl salt under Cl_2 bubbling which needs to be further investigated.

ACKNOWLEDGMENT

The authors would like to acknowledge Dr.K. Nagarajan and Dr.B. Prabhakara Reddy of Radio Chemistry Lab, IGCAR, Kalpakkam for the help and support in conducting the experiments.

REFERENCES

1. Baldev Raj, H.S. Kamath, R. Natarajan and P.R. Vasudeva Rao, “A perspective on fast reactor fuel cycle in India,” *Prog. Nucl. Energy* 47, (2005): p. 369.

2. Y.S. Li, M. Spiegel, S. Shimada, “Corrosion behaviour of various model alloys with NaCl – KCl coating,” *Mater. Chem. Phys* 93, (2005): p. 217.

3. M.A. Uusitalo, P.M.J. Vuoristo, T.A. Mantyla, “High temperature corrosion of coatings and boiler steels below chlorine-containing salt deposits,” *Corros. Sci* 46, (2004): p. 1311.

4. M. Asou, S. Tamura, T. Namba, H. Kamoshida, Y. Shoji, K. Mizuguchi, T. Kobayashi, “The Corrosion Resistance Tests of Crucible Materials for the Oxide Pyro-Process”, Proceedings of GLOBAL 1999 Conference, held at Jackson hole, Wyoming, USA, Aug 29-Sep 3, 1999.

5. A. Takeuchi, T. Kato, K. Hanada, T. Koizumi, S. Aose, “Corrosion resistance of ceramic materials in pyrochemical reprocessing condition by using molten salt for spent nuclear oxide fuel,” *J. Phys. Chem. Solids* 66, (2005): p. 521.

6. ASTM Standard G28-02, “Standard Test Methods of Detecting Susceptibility to Intergranular Corrosion in Wrought, Nickel-Rich, Chromium-Bearing Alloys” (USA: ASTM International, 2002) p. 1.

7. Powder Diffraction File-2 (PDF-2) JCPDS-ICDD, PCPDFWIN Version 2.02, May 1999.

8. J.E. Indacochea, J.L. Smith, K.R. Litko, E.J. Karell, and A.G. Raraz, “High-temperature oxidation and corrosion of structural materials in molten chlorides, Oxidation of metals,” *Oxid. Met* 55, (2001): p. 1.

9. N. Birks, G.H. Meier, F.S. Pettit, *Introduction to the High Temperature Oxidation of Metals*, 2nd ed. (UK: Cambridge University Press, 2006), p. 149.

10. ASM Handbook, Vol. 13A: Corrosion: Fundamentals; Testing and Protection, (Metals Park, OH: ASM International, 2003), p. 216.

11. J.H. DeVan, “Catastrophic Oxidation of High-Temperature Alloys”, Oak Ridge National Laboratory Report, Report No: ORNL-TM-51, 1961.

12. K.R. Peters, D.P. Whittle, J. Stringer, “Oxidation and hot corrosion of nickel-based alloys containing molybdenum,” *Corros. Sci* 16, (1976): p. 791.

13. E.H. Kim, J.H. Lee, S.H. Cho, J.K. Oh, H.S. Lee, S.W. Park, “Development of a corrosion resistant structural material in an electroreducer”, Proceedings of International Pyroprocessing Research Conference, held at Republic of Korea, Aug 24-27, 2008.

14. A. Ravi Shankar, S. Mathiya, K. Thyagarajan and U. Kamachi Mudali, “Corrosion and Microstructure Correlation on Materials in Molten LiCl-KCl Medium,” *Metall. Mater. Trans A* 47, (2010): p. 1815.

15. A. Ravi Shankar, A. Kanagasundar, U. Kamachi Mudali, “Corrosion of Nickel Containing Alloys in Molten LiCl-KCl Medium,” *Corrosion* 69, (2013): p. 48.

16. A. Ravi Shankar, U. Kamachi Mudali, “Corrosion of 316L Stainless Steel in Molten LiCl-KCl Salt,” *Mater. Corros* 59, (2008): p. 878.

17. A. Ravi Shankar, K. Thyagarajan and U. Kamachi Mudali, “Corrosion Behaviour of Candidate Materials in Molten LiCl-KCl Salt Under Argon Atmosphere,” *Corrosion* 69, (2013): p. 655.

18. S.H. Cho, J.M. Hur, C.S. Seo, S.W. Park, “High temperature corrosion of superalloys in a molten salt under an oxidizing atmosphere,” *J. Alloy. Compd* 452, (2008): p. 11.

19. R. Bender, M. Schütze, “The role of alloying elements in commercial alloys for corrosion resistance in oxidizing-chloridizing atmospheres. Part I: Literature evaluation and thermodynamic calculations on phase stabilities,” *Mater. Corros* 54 (2003): p. 567.

20. A. Ruh, M. Spiegel, “Thermodynamic and kinetic consideration on the corrosion of Fe, Ni and Cr beneath a molten KCl–ZnCl2 mixture,” *Corros. Sci* 48 (2006): p. 679.

21. G.Y. Lai, Molten salt corrosion in: High temperature corrosion of engineering alloys, ASM International, p.169.

22. R. Bender, M. Schütze, “The role of alloying elements in commercial alloys for corrosion resistance in oxidizing-chloridizing atmospheres. Part II: Experimental investigations,“ *Mater. Corros* 54 (2003): p. 652.

23. A. Ravi Shankar, U. Kamachi Mudali, Ravikumar Sole, H.S. Khatak and Baldev Raj, “Plasma-sprayed yttria-stabilized zirconia coatings on type 316L stainless steel for pyrochemical reprocessing plant,” *J. Nucl. Mater* 372, (2008): p. 226.